A new theoretical technique for the measurement of high-frequency relic gravitational waves

R. Clive Woods[1], Robert M L Baker, Jr.[2], Fangyu Li[3], Gary V. Stephenson[4], Eric W. Davis[5] and Andrew W. Beckwith[2]

[1] Department of Electrical and Computer Engineering, Louisiana State University, Baton Rouge, LA 70803-5901, USA
[2] GravWave® LLC and Transportation Sciences Corporation, 8123 Tuscany Avenue, Playa del Rey, CA 90293, USA
[3] Department of Physics, Chongqing University, Chongqing 400044, People's Republic of China
[4] Seculine Consulting, PO Box 925, Redondo Beach, CA 90277, USA
[5] Institute for Advanced Studies at Austin, 11855 Research Boulevard, Austin, TX 78759, USA

Abstract It is generally accepted that under most models of the early universe evolution, high-frequency gravitational waves (HFGWs) were produced. They are referred to as "relic" high-frequency gravitational waves or HFRGWs and their detection and measurement could provide important information on the origin and development of our Universe – information that could not otherwise be obtained. So far three instruments have been built to detect and measure HFRGWs, but so far none of them has achieved the required sensitivity. This paper concerns another detector, originally proposed by Baker in 2000 and patented, which is based upon a recently discovered physical effect (the Li effect); this detector has accordingly been named the "Li-Baker detector." The detector has been a joint development effort by the P. R. China and the United States HFGW research teams. A rigorous examination of the detector's performance is important in the ongoing debate over the value of attempting to construct a Li-Baker detector and, in particular, an accurate prediction of its sensitivity will decide whether the Li-Baker detector will be capable of detecting and measuring HFRGWs. Its sensitivity and noise sources as well as other operational concerns are discussed here. The potential for useful HFRGW measurement is theoretically confirmed.

Keywords: high-frequency gravitational waves; high-frequency relic gravitational wave measurement; primordial gravitational waves; microwaves; cosmology; general relativity

PACS numbers: 95.55.Ym, 98.70.Vc, 98.80.Es, 85.70.ay, 04.30.Nk, 04.25.Nx, 04.30.Db, 04.80.Nn

1 Introduction

Most models of early universe evolution predict that high-frequency gravitational waves (HFGWs) were produced as a result of the violent expansion of the young universe. These HFGWs are referred to as primordial or "relic" high-frequency gravitational waves (HFRGWs) and their measurement and characterization could provide important information on the origin and development of our Universe since their properties were uniquely determined by the most violent event in the history of the Universe. This information is a vital piece in the jigsaw of understanding how the young universe evolved, and that information cannot be obtained by any other means. A number of techniques have been proposed for measuring relic GWs at both low

frequency and high frequency, and some GW detectors have been built, so far without any success in detection. Like the Laser Interferometer Space Antenna (LISA) [1], the swarm of Cosmic Microwave Background (CMB) sensors [2] and the Russian gravitational-electromagnetic resonance high-frequency gravitational wave detector [3,4] (all proposed for sensing primordial or relic gravitational waves), no Li-Baker detector has yet been constructed.

As is well known, Einstein [5] predicted the possibility of waves in four-dimensional spacetime, i.e., the usual three dimensions of space plus time. These waves are gravitational waves whose spacetime strain is h. This spacetime strain is analogous to mechanical strain in a beam, and is the ratio of the change in length to the original length (without the stress of a passing gravitational wave). Thus, the strain, h, has units of meters per meter (m/m) and is dimensionless. The spacetime strain is a function of position and time and its RMS value is h_{rms} and the local value at a detector is h_{det}.

The importance of measuring the HFRGW strain h and dimensionless energy density Ω_{gw} is that predictions of their values produced by the "Big Bang" under inflationary universe models [6-11] and cosmological string scenarios [12-14] are available, and so direct measurement will allow discrimination between the various models. Many of these models predict maximum HFRGW amplitude around 10GHz, with h in the approximate range 10^{-30} to $\sim 10^{-34}$. Low-frequency gravitational wave detectors such as LIGO, based upon optical interferometers, have an optimal detection frequency ~100 Hz with upper frequency detection limit of ~2000Hz, and accordingly cannot detect HFRGWs [15]. The proposed laser interferometer space antenna (LISA)[1] gives optimal performance in the range $\sim 10^{-6}$ to 10^{-2} Hz. In order to detect and measure high frequencies at small amplitudes, detectors utilizing different techniques must be employed, complementary to the low frequency detectors. Krauss, Scott and Meyer [2] suggest "… primordial (relic) gravitational waves also leave indirect signatures that might show up in CMB (Cosmic Wave Background) maps." They propose the use of thousands of new detectors (possibly as many as 50,000) as well as spacecraft-borne detectors to obtain the required sensitivity.

Theorized cosmological signatures (i.e., frequency spread, polarization and phase) of the HFRGWs are important because of the uncertainty surrounding cosmological parameters leading to variations in the early universe [16]. One of the most important parameters for analysis of the beginning of the Universe is the dimensionless relic gravitational wave energy density, Ω_{gw} [10, 17-20]. According to these estimates, the upper limit of Ω_{gw} for relic GWs should be smaller than 10^{-5}. In fact, recent estimates [1] show that the upper limit of Ω_{gw} should be 6.9×10^{-6} at about 100 Hz. The spectra of dimensionless primordial relic GW strains h and h_{rms} as a function of frequency have been estimated in detail by Grishchuk [10, 17-20]. Detailed observational data for h and its variation in time and direction can be used to refine the estimated value of Ω_{gw}, and hence to differentiate among the competing cosmological theories for the beginning of the Universe.

Three high-frequency gravitational wave (HFGW) detectors have been built [21] and another has been proposed [3, 4], all utilizing different measurement techniques. These are promising for future detection of HFRGWs having frequencies above 100 kHz (the definition of HFGWs adopted by Douglass and Braginsky [22]), but their sensitivities are each many orders of magnitude less than that required to detect and measure primordial HFRGWs.

The first of these detectors has been constructed at Birmingham University, England. The Birmingham HFGW detector measures changes in the polarization state of a microwave beam

(indicating the presence of a GW) moving in a waveguide [23, 24]. It is expected to be sensitive to HFRGWs having spacetime strains of $h \sim 2 \times 10^{-13}$.

The second detector, built at INFN Genoa, Italy. It is a resonant HFRGW detector, comprising two coupled, superconducting, spherical, resonant chambers a few centimeters in diameter and configured as oscillators. The oscillators are designed to have (when uncoupled) almost equal resonant frequencies and when the frequency of the HFGW is just equal to the frequency difference between the normal modes in the two coupled spherical cavities, the EM energy conversion between the cavities will be maximum and the HFGW sensed. The system is expected to have a sensitivity to HFRGWs of about $h \sim 2 \times 10^{-17}$with future expectation of $\sim 2 \times 10^{-20}$ [25-27]. However, there is no further planned development of the INFN Genoa HFRGW detector.

The third detector is the Kawamura 100 MHz HFRGW detector that has been built by the Astronomical Observatory of Japan. It comprises two synchronous interferometers having arms lengths of 75 cm. Its sensitivity is $h \approx 10^{-16}$, projected to improve to $\sim 10^{-27}$ [28]. It appears that due to the size of the instrument it will be difficult for this design to operate satisfactorily at 10GHz with their projected sensitivity.

Another HFGW detector, under development at the Steinberg Astronomical Institute in Russia [3, 4] detects gravitational waves by their action on an electromagnetic wave in a closed waveguide or resonator.

An objective of this paper is to present the rationale behind a proposed and planned HFRGW detector utilizing a new measurement technique termed the "Li effect." This theory was first published in 1992 [29]. Subsequently, the Li effect has been developed further in nine later peer-reviewed research papers [30-38] and is scrutinized by Valentine Rudenko and Nikolai Kolosnitsyn of the Sternberg Astronomical Institute of Moscow State University. The key results are summarized in ref. [37] and a detailed discussion of the detection mechanism is given in ref. [38] and presented in compact form in the Appendix.

This new detection technique is based upon coupling between an HFGW, a Gaussian-type microwave photon beam (having the same frequency, direction and suitable phase as the HFRGW being detected), and a static magnetic field. The result of this coupling is a flux of detection photons or perturbative photon flux (PPF), and reflectors would typically be used to direct the PPF towards sensitive microwave receivers [39]. Exploitation of the Li effect to produce a HFGW detector was first conceived by Baker in 2000, and a detector based upon this principle is therefore called the Li-Baker detector and was patented in China [40]. First estimates of its sensitivity in the microwave band have been similar to those needed for detection of primordial HFRGW [11, 18, 37, 38]. There are, however, operational concerns such as fundamental noise sources that must be examined. Sources of noise in this detector include: background photon noise from the Gaussian microwave beam including diffraction, thermal noise from the detector's containment vessel, dark-background shot noise, Johnson noise in the microwave receivers, preamplifier noise, and quantization noise.

In the Li-Baker-detector the key parameter is the first-order detection photons (proportional to sine wave GW strain amplitude A), or perturbative photon flux (PPF), and not the second-order PPF (proportional to A^2). The first-order PPF, or the flux of detection photons produced by the Li-effect interaction with the GWs, is therefore proportional to $\sqrt{\Omega_{gw}}$ and not Ω_{gw}. The spectra predicted by the pre-big-bang models (figure 2 of [1]) shows that Ω_{gw} of relic GWs is

almost constant at 6.9×10^{-6} in the frequency range = 10 Hz to 10 GHz. Cosmic string models predict $\Omega_{gw} \sim 10^{-8}$ in the range 1 Hz to 10 GHz; its peak value is at about 10^{-7} to 10^{-6} Hz, in the low-frequency regions – much lower than HFGW frequencies. LISA might achieve the requisite sensitivity for detection of relic GWs expected from cosmic string models in the range 10^{-6} to 10^{-2} Hz. Also, it is shown [1] that only the Advanced LIGO may achieve the requisite sensitivity for relic GWs predicted by the pre-big-bang model in the frequency band around ~100 Hz; the present LIGO cannot detect relic GWs in that region. However, the Li-Baker detector could make observations of h at around 10 GHz and, unlike the current Low-Frequency Relic Gravitational Wave (LFRGW) detectors, could be sensitive enough to measure relic gravitational waves. Furthermore, with the dimensionless-cosmological Hubble parameter n = 1.0 and 1.2, there are sharp peaks of Ω_{gw} at 10 GHz [41] as shown in Fig. 1. Grishchuk's analyses that define these peaks are too lengthy to be included here, but can be found in Refs. [10, 17-20]. A frequency scan, discussed in section 3.5, could reveal other HFRGW effects of interest in the early universe at a variety of HFRGW base frequencies other than 10 GHz.

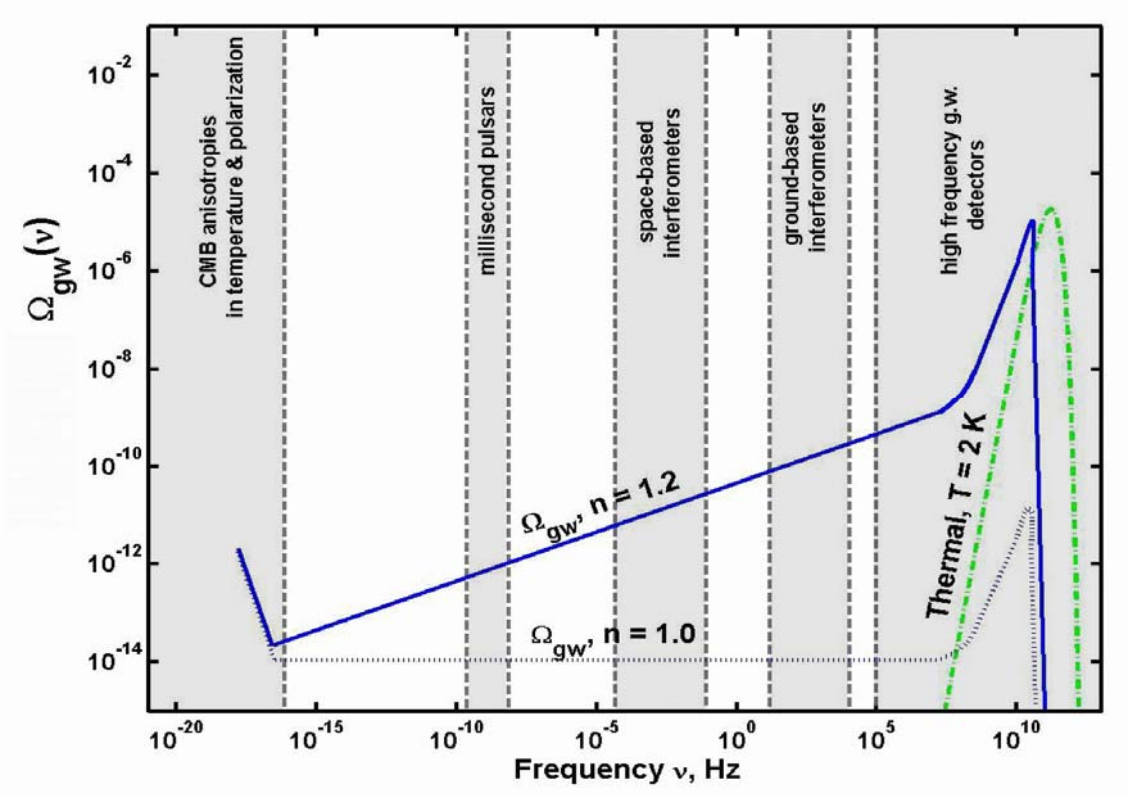

Figure 1. Predicted relic gravitational wave energy density as a function of frequency (slide 6, [41]).

2 Electromagnetic and gravitational wave interaction: the Gertsenshtein and Li effects

The Li Effect is *very different* from the well-known classical *(inverse)* Gertsenshtein effect [42], in which a GW travelling in a region in which there is a uniform constant applied magnetic field will produce a coupled electromagnetic (EM) wave having exactly the same frequency and wave-vector as the incoming GW. By contrast, in the Li effect, an electromagnetic (EM) wave of a Gaussian beam (GB) in the presence of a perpendicular static magnetic field is found to interact with an incoming GW having exactly the same frequency and wave-vector (including the direction of propagation) as those of the EM wave. This is known as the "*synchro-resonance condition,*" which may typically be satisfied by one Fourier component of a continuous spectrum of incoming GWs. This interaction produces a *resultant second EM wave of the same frequency as the EM and GW waves, but propagating perpendicular to both the applied uniform magnetic field and to the applied EM wave*, as shown in Fig. 2. It is *unlike* the (inverse) Gertsenshtein effect, in which the resultant EM wave is parallel to (rather than perpendicular to) the incoming GW, and in which there is no applied EM wave used to synchronized to the incoming GW. In the Li effect, the perpendicularly emitted photons signal the presence of HFGWs and are termed the "perturbative photon flux," or PPF. A practical GW detector based upon this principle will need to detect the PPF using EM or microwave techniques to signify the presence of GW.

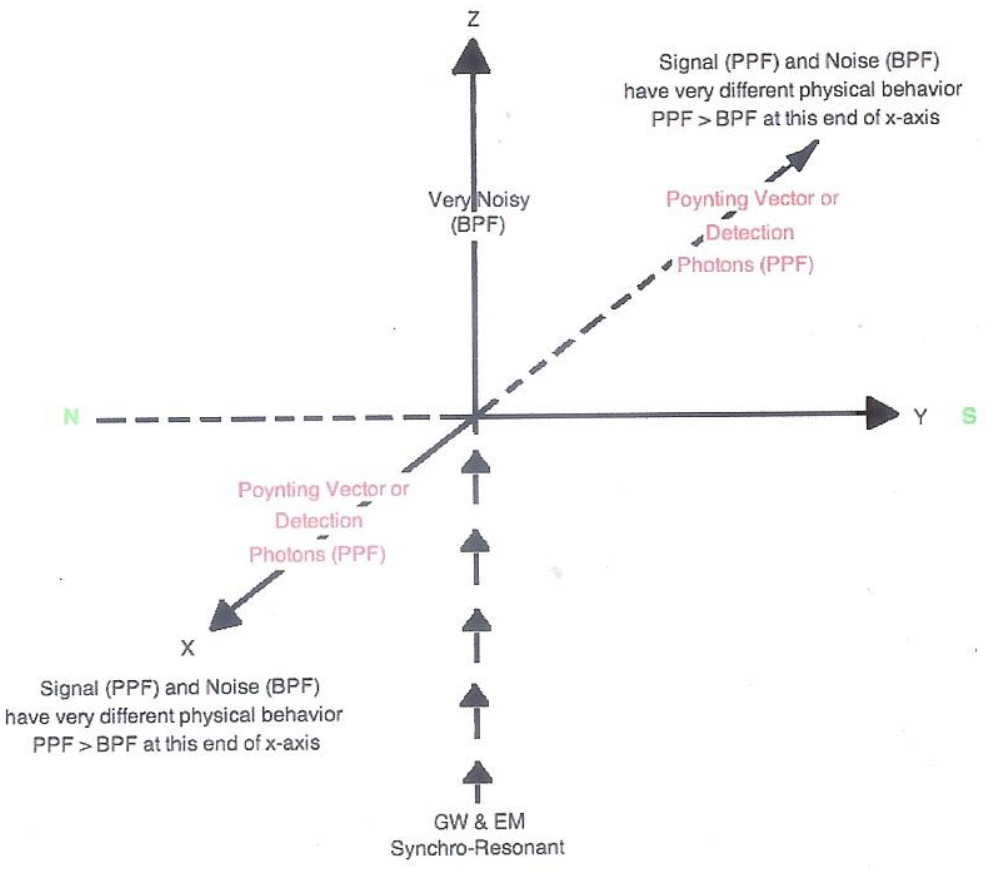

Figure 2. Li effect PPF directed to the ends of the *x*-axis

Thus, the PPF is distinguished from the applied EM wave by its different propagation direction, and it must be received at a location (or locations) relatively free from extraneous EM noise. The perpendicular propagation direction of the PPF is a *fundamental physical requirement*; otherwise the EM fields will not satisfy the Helmholtz equation, the electrodynamics equation in curved spacetime, the non-divergence condition in free space, and the laws of energy conservation as discussed in the Appendix and in [33]. A significant feature of the Li-effect is that the PPF move both outward away from the GB's axis and *inward* toward the GB's axis. Thus reflectors *in* the GB itself can reflect and focus a portion of the PPF to microwave receivers in regions of the detector proper that are relatively noise free. The BPF noise, whatever its source (except for scattering as discussed in section 4), *mainly propagates radially out* from the GB's axis and is *not* focused to the microwave receivers.

3. Description of Li-Baker HFGW detector and its physical parameters

3.1 *Gaussian beam*

A Gaussian microwave beam (GB) is used as the applied EM wave required in the Li effect. It is to be produced by a conventional microwave transmitter with its antenna aimed along the +*z*-axis of Fig. 2. Its frequency and direction are the same as the frequency and direction of the incoming HFGW signal that will be detected [43] as shown in Fig. 3. The GB frequency is expected to be typically around 10 GHz for GB directed along the +*z*-axis will allow detection of a HFRGW also directed along the +*z*-axis.

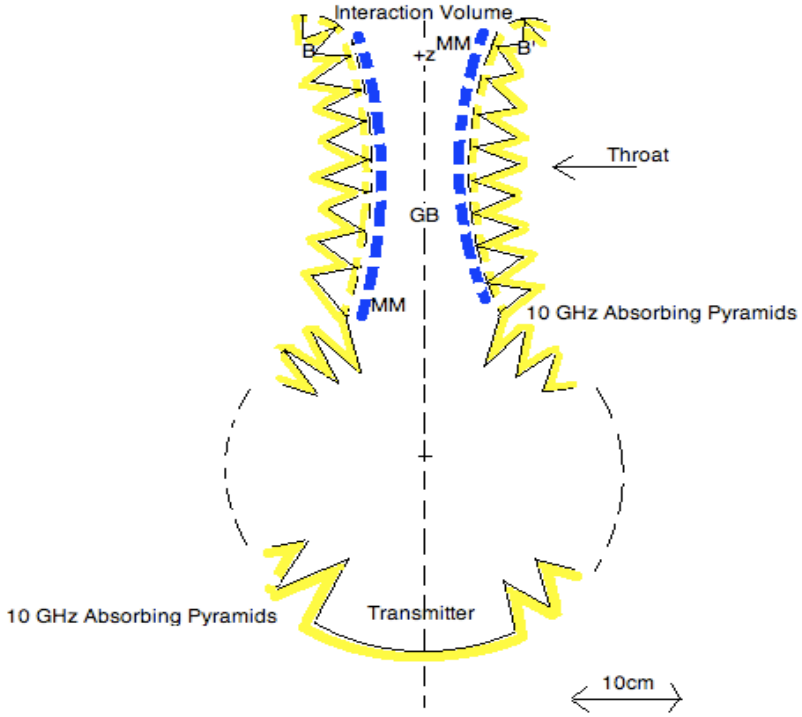

Figure 3. Gaussian-beam transmitter compartment

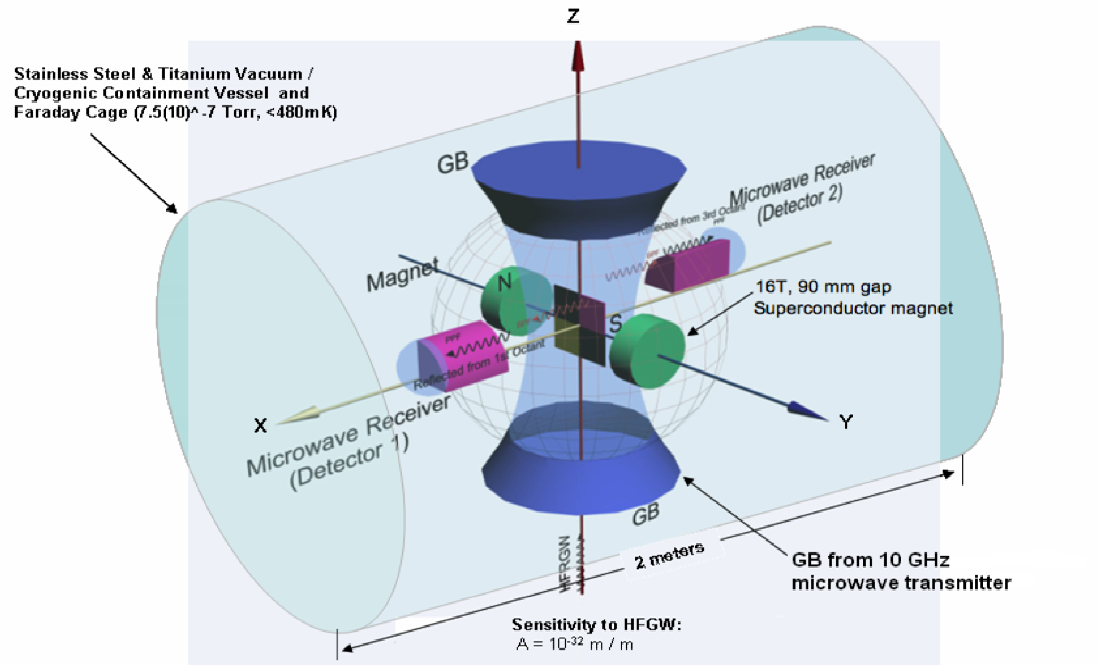

Figure 4. Schematic of the Li-Baker HFGW detector

In order to reduce the thermal load on the refrigeration system the microwave transmitter and main GB microwave absorber are in separate chambers sealed off from the main detector chamber by microwave transparent walls. A high-vacuum system able to evacuate the chamber from 10^{-6} to 10^{-11} Torr (nominally about 7.5×10^{-7} Torr) is needed to allow cryogenic operation and to reduce thermal noise (see section 4)

3.2 *Magnetic field and sensitivity*

A static magnetic field **B** (generated typically using one or more superconducting magnets (such as those found in a conventional MRI medical body scanner) is directed along the *y*-axis, as shown schematically in Fig. 4. Rather than using one pair as shown schematically in Fig. 4, it may be more cost-effective to use a number of magnet pairs spaced equally in the z-direction. The intersection of the magnetic field and the GB defines the "interaction volume" where the PPF is produced and move out in both x directions on both sides of the y-z-plane (as in Fig. 2.A of the Appendix). The interaction volume in the GB for the proposed or nominal design is roughly cylindrical in shape, about 30 cm in length and about 9 cm cross-section diameter. In order to estimate the *detection signal*, or the number of detection photons (PPF) produced per second for a given amplitude HFGW, we will utilize equation (7) of the analyses in [44], which is a simplification of equation (59) in [32] for a near-field approximation as discussed in [44],

$$n_x^{(1)} = [1/(\mu_0 \hbar \omega_e)]\, AB_y\psi_0\delta s \qquad (3.1)$$

where $n_x^{(1)}$ is the number of x-directed detection photons per second produced in the interaction volume, $\hbar$ = Planck's reduced constant, ω_e = angular frequency of the EM wave (= $2\pi\nu_e$), ν_e = frequency of the EM wave, A = the HFGW amplitude (the dimensionless strain of spacetime variation with time), B_y = y-component of the magnetic field, ψ_0 = electrical field of the EM Gaussian beam and δs is the cross-sectional area of the interaction volume perpendicular to the PPF. For the proposed nominal design, the minimum cross-section diameter or waist of the GB is located about 20 cm away from the antenna; the radius of the GB at its waist, W, is $(\lambda_e z/\pi)^{1/2} = 4.4$ cm at 10GHz, so that its diameter is 8.8 cm (approximately the width of the interaction volume); and the length of the interaction volume is l = 30 cm, so $\delta s = 2Wl = 2.58 \times 10^{-2}$ m^2. From the analysis presented in ref. [30], the electrical field of the EM GB, ψ, is 1.26×10^4 Vm^{-1} for transmitter power 1kW. For the present proposed design, $\nu_e = 10^{10}$ s^{-1}, $\omega_e = 6.28 \times 10^{10}$ rad/s , $A = 10^{-30}$, and $B_y = 16$ T. Thus (3.1) gives $n_x^{(1)} = 99.2$ PPF detection photons per second. For a 10^3 second observation accumulation time interval, there would be about 10^5 detection photons created (the PPF). About one-fourth of them would be focused at each receiver, since half would be directed towards $+x$ and half directed towards $-x$ on each side of the focusing reflectors in the y-z plane (only the half of the photons directed toward the reflectors is focused to the microwave receivers the other half is directed away from the reflectors and unfocused and does not reach the receivers). Table 1 provides values for an interaction volume cross section of δs = 0.1 m × 0.05 m = 0.005 m^2 (a very small detector), Table 2 is for δs = 0.30 m × 0.088 m = 0.0258 m^2 (the proposed or nominal design) and Table 3 is for δs = 6 m × 0.5 m = 1.5 m^2 (a large detector design). Table 3 is valid under the assumption that the near–field approximation of (3.1) still holds and account is taken of the spreading property of the GB. If the interaction volume is very large in one direction, for example much greater than 1m, then the computation of the total PPF could be somewhat more accurately obtained by an integration of equation (59) of [32], specifically, the numerical integration of the coefficients in equations (60) of [32]. In such a case the evacuation pressure would also need to be somewhat lower in order to increase the GB photon mean free path and minimize GB photon scattering (see Section. 4). Such a refinement is not judged to be necessary so the approximation of (3.1) was utilized in Table 3.

Unlike the Gertsenshtein effect, the Li effect produces a *first-order* PPF whose amplitude is proportional to the incoming gravitational wave (GW) amplitude A as in (3.1) (and is not a second-order effect proportional to A^2). In the inverse Gertsenshtein effect, the EM wave produced is a second-order effect; from equation (7) in [33], the number of EM photons produced in the inverse Gertsenshtein effect is "…proportional to the amplitude squared of the relic HFGWs, A^2," and it would be necessary to accumulate such EM photons for at least 1.4×10^{16} seconds or 444 million years in order to achieve HFRGW detection utilizing the inverse Gertsenshtein effect as computed in [33]. Since in the Li effect the number of EM photons is proportional to the amplitude of the relic HFGWs, which is typically $A \approx 10^{-30}$, not its square, so that it would be necessary to accumulate such EM photons for only about 10^2 to 10^5 seconds in the transverse background photon noise fluctuation in order to achieve relic HFGW detection as computed in [33]. The JASON report [45] confuses the two effects and erroneously suggests that the Li-Baker HFGW detector utilizes the inverse Gertsenshtein effect. The Li-Baker HFGW detector does *not* utilize the inverse Gertsenshtein effect, and it has a theoretical sensitivity that is about $A/A^2 = 10^{30}$ greater than the value incorrectly reported in the JASON report [43A] for HFRGWs.

Table 1. PPF (photons per second) for various values of B_y and transmitter power for $\delta s = 0.005$ m^2.

	Power = 100 W	Power = 1000 W	Power = 10,000 W
$B_y = 9$ T	3.4	10.8	34.2
$B_y = 16$ T	6.1	19.2	60.8
$B_y = 20$ T	7.6	24	76

Table 2. PPF (photons per second) for various values of B_y and transmitter power for $\delta s = 0.0258$ m^2. The design or nominal case.

	Power = 100 W	Power = 1000 W	Power = 10,000 W
$B_y = 9$ T	17.6	55.8	176.4
$B_y = 16$ T	31.4	**99.2**	313.7
$B_y = 20$ T	39.2	124	392

Table 3. PPF (photons per second) for various values of B_y and transmitter power for $\delta s = 1.5$ m^2.

	Power = 100 W	Power = 1000 W	Power = 10,000 W
$B_y = 9$ T	1.023×10^3	3.2×10^3	1.026×10^4
$B_y = 16$ T	1.83×10^3	5.8×10^3	1.82×10^4
$B_y = 20$ T	2.3×10^3	7.2×10^3	2.3×10^4

For an advanced Li-Baker detector [35], also included would be a resonance chamber ($Q \sim 10^3$) in the interaction volume, and more sensitive microwave receivers so that the sensitivity could be further improved. These refinements will be considered elsewhere.

3.3 *Microwave reflectors*

Semi-paraboloid reflectors are situated back-to-back in the *y-z* plane of the GB, as shown in Figs. 5 and 6, to reflect the $+x$ and $-x$ propagating PPF to the microwave receivers. The effective aperture of each reflector is 60cm and the sagitta or depth of curvature of such a mirror is about 2.26 cm. Since this is greater than one tenth of a wavelength of the PPF, $\lambda_e/10 = 0.3$ cm, such a paraboloid reflector is desirable rather than only a tilted plane mirror. As discussed in Section 4, for elimination of any diffracted photons emanating from the GB's entrance to the main detector chamber at ***B – B'*** of Fig. 5, the reflector's focus is below the x axis and "out of sight" of the GB's entrance. Thus the diffracted photons waves from the GB entrance will have at least one reflection from the absorbent detector walls prior to reaching the microwave receivers. As will be calculated in section 4 other radiation from the GB due to scattering and the natural fall off of GB radiation in the radial direction is negligible, so that the BPF is only due to diffraction from the transmitter's antenna, aperture or entrance to the main detector chamber. This is why the paraboloid mirrors are slightly tilted, which allows the focus to be slightly below the *x-y* plane (similar to a Herschelian optical telescope) so that there is no direct straight line between the microwave receivers and the transmitting antenna. Since such a reflector would extend out 2.26 cm into the GB (on both sides of y-z plane or 4.5 cm in total), a half or semi-paraboloid mirror is used instead in order not to block the Gaussian beam significantly. In the nominal case the reflectors are about 30 cm high (along the z-axis) and 9 cm wide (along the y-axis) and extend

from z = 0 cm to z = +30 cm as shown in the figures. The reflectors can be installed *inside* the GB in order that the diffracted BPF from the GB transmitter's entrance to the detector chamber at **B** – **B'** and any diffraction perpendicular to the GB will *not* be directly focused onto the receivers. The only photons reflected or focused onto the microwave receivers will be the ± x-directed PPF photons *in the* GB *that are directed toward the* GB's *center* (there could be several microwave receivers stacked at each end of the x-axis to in increase the field of view and *account for any variations in the magnetic field from uniform straight lines*). The semi-paraboloid reflectors are tilted "down" at about ½ (3 cm/ 100 cm) = 0.015 radians (about 0.86^0) or more (in order to focus at receivers 100 cm distant and 3 cm below the base of the GB) and extend from a sharp edge at point ***A*** at the center of the GB, which is totally shielded from the receivers, as shown in Fig. 5. Thus there will be very little blockage of the GB. The reflectors can be constructed of almost any material that is non-magnetic (to avoid being affected by the intense magnetic field), reflects microwaves well and will not outgas in a high vacuum. The material of the reflectors can be in the form of fractal membranes that reflect more than 99 % of the incident microwaves (experimental data from figure 1c of [46]). Apparently the fractal membranes (which consist of printed microcircuits) produce little diffraction in the presence of the GB and in the base frequency range pass all the remainder radiation through the fractal membranes **[**47**].** Alternatively, microwave focusing lenses can be placed outside of the GB on either side [39] as in Fig. 7.

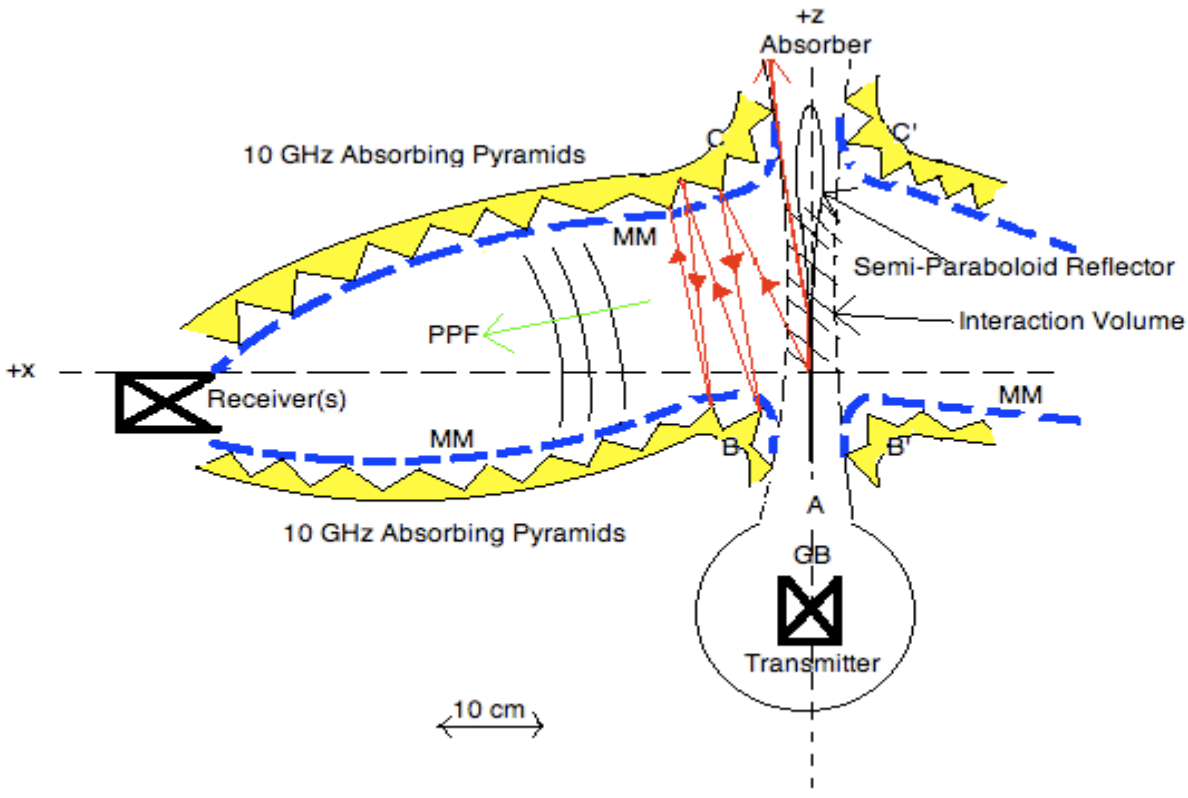

Figure 5. Side-view schematic of the Li-Baker HFGW detector, showing microwave-absorbent walls in the anechoic chamber and, if not totally absorbed, also showing the paths of reflected, diffracted photons.

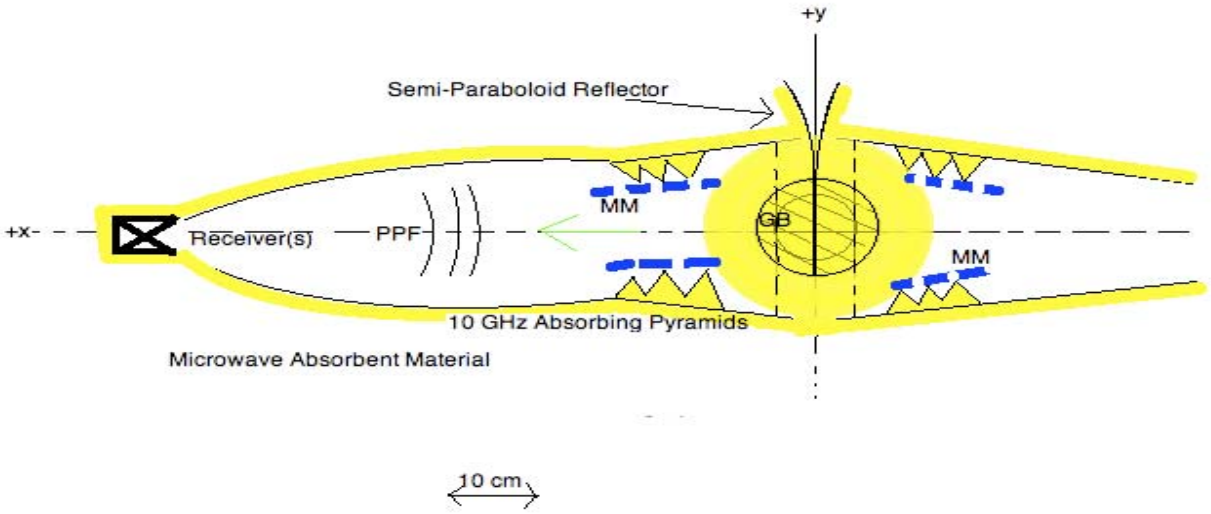

Figure 6. Plan-view schematic of the Li-Baker HFGW detector, exhibiting microwave-absorbent walls in the C and the reflectors extending out on either side of the x-axis along y with edges completely shielded from the receivers

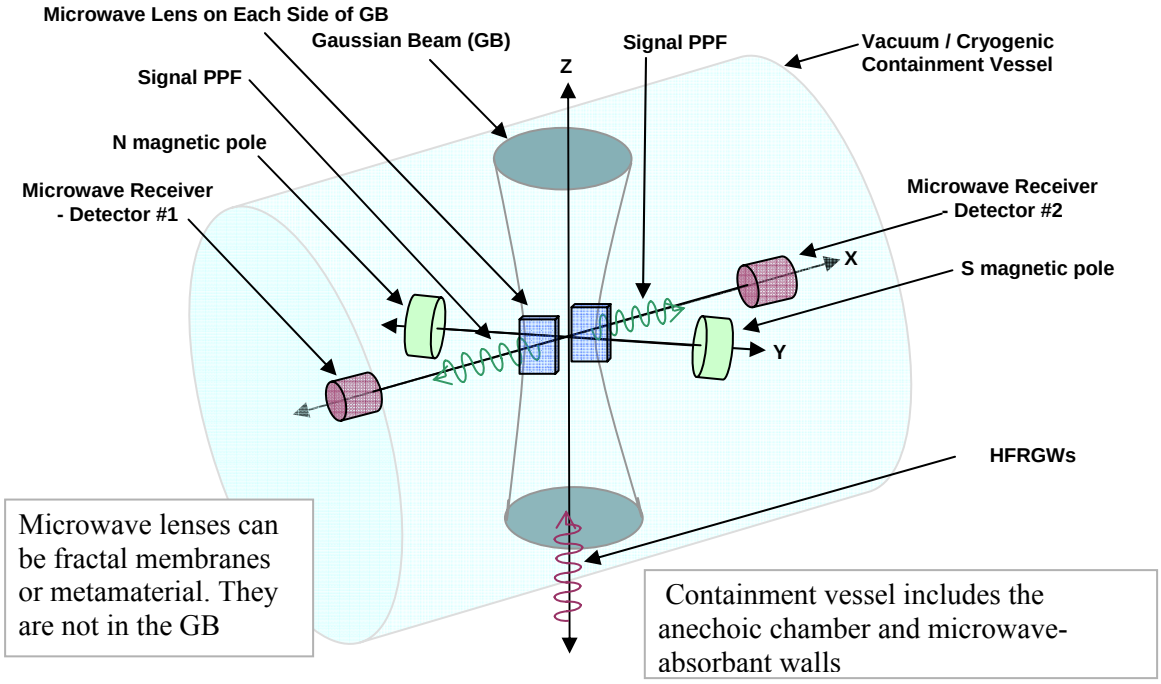

Figure 7. Schematic of the Li-Baker HFGW detector, exhibiting microwave lenses on each side of the GB focusing PPF on the microwave receivers.

3.4 *Microwave receivers*

High-sensitivity~~,~~ shielded microwave receivers are located at each reflector focal point. Possible receiver technologies to use include a microwave horn plus HEMT (High Electron Mobility Transistor) receiver; a Rydberg Atom Cavity Detector [48]; a quantum electronics device (QED) microwave receiver, such as the Yale detector invented by Schoelkopf and Girvin [49**]**, and a single-photon detector~~s~~ [50]. Of these, the HEMT receiver is most likely for initial trials because of its off-the-shelf availability from many suppliers. The synchro-resonant condition specifies that the GW detected has the same frequency and propagation direction as the GB. In order to achieve a larger field of view and *account for any curvature in the magnetic field*, an array of microwave receivers having, for example, four 3 cm × 3 cm horns could be installed parallel to the *y*-*z* plane and 9 cm below the GB's base.

3.5 *Bandwidth*

The "detected bandwidth" (BW) is determined by two factors:

- random fluctuations in the GB transmitter output causing BW broadening, and
- the bandwidth of the microwave receivers. In general, the narrower the frequency range or bandwidth is the more sensitive is the detector (the noise floor is lowered at smaller BW).

However, frequency scanning allows a wide band of HFRGWs to be analyzed. As an example, in a 1 Hz "bandwidth" and a 1000s observation interval, then over a year of observation about 30kHz HFRGW frequency band could be scanned. Essentially one would sample the detected BW by a number of very narrow actual bandwidths, B_w. If the observation interval is 1000s, then the actual B_w is 0.001Hz. or, for 100s observation interval, then a 300 kHz band of HFRGWs could be scanned. For a 1 kHz BW, then a 0.3 GHz band could be scanned using 100s intervals over a year, and this would be a substantial BW if centered on 10GHz base frequency.

4. Noise

Many of the noise sources in the Li-Baker HFGW detector are similar to those encountered in any microwave receiver, and may be analyzed in similar fashion. The difference is that the HFRGW signal manifests itself as detection photons (PPF) created by the interaction of a microwave beam (GB) and the GWs. The presence of the microwave beam having the same frequency as the detection photons gives rise to background photon flux (BPF) that produces *dark-background shot noise* in addition to the usual microwave receiver noise. For example, *Johnson noise* originates thermally in any electrical resistor, and is often dominated by the contribution of the most significant resistance in the receiver input stage. In order to account for all these diverse noise sources, here they are translated through the detector to the actual microwave receiver(s) and termed *noise equivalent power* or NEP [51**]**. Photon noise from the GB will be considered in detail since it is likely to be the dominant source of noise in the Li-Baker detector.

4.1 *Noise generated by the GB*

The intensity of the GB is written (equation (3) of [34]) and is:

$$n_z^{(0)} \sim \exp(-2r^2 / W^2); \tag{4.1}$$

where r is the radial distance out from the GB's axis and W is the radius of the GB at its waist. The transverse BPF in any longitudinal symmetrical surface of the GB must vanish. Even if we treat a non-idealized situation, there are always the special local regions in which the transverse BPF vanish. If the transverse BPF in any longitudinal symmetrical surface of the GB is not vanishing, then the photon number at the symmetrical surface will be continuously accumulated (increased) with time in "the imploding wave" region of the GB and continuously reduced (decreased) with time in the "outgoing wave" region of the GB. Thus the "stability" of the GB would be destroyed (see figure 2 and figure 4 on p. 414 of [37]). In the prototype Li-Baker HFRGW detector under analysis, which has peak sensitivity (base frequency) at 10 GHz, the energy per detection photon is $\hbar\, v_e = 6.626 \times 10^{-24}$ J, while the HFRGWs or the GB both have the same frequency for synchro-resonance. So a 10^3 W GB contains 1.51×10^{26} photons/s. For 100-cm-distant microwave receivers, the GB intensity in the z-direction, if (4.1) is accurate at such large attenuations, is reduced to $\exp(-2\times100^2/4.4^2)(1.51 \times 10^{26})$, which is essentially zero.

With regard to molecular scattering in the GB, we utilize the Rayleigh scattered intensity of microwave photons, I, from a molecule with incident photon intensity I_o as given by [52]

$$I = I_o \frac{8\pi^4\alpha^2}{\lambda^4 R^2}(1+\cos^2\theta) \tag{4.2}$$

in which α is the atomic polarizability expressed as a polarization volume (where the induced electric dipole moment of the molecule is given by $4\pi\varepsilon_o\alpha E$), θ is the scattering angle, and R is the distance from particle to detector. Note that the scattering is not isotropic (there is a θ-dependence), but in the present case, $\theta = 90°$ so the ratio of incident to scattered photon intensity is given by $\frac{8\pi^4\alpha^2}{\lambda^4 R^2}$. The polarizability is $\alpha \approx 1.1 \times 10^{-30}$ m^3 from [53] so the scattering intensity ratio is 1.2×10^{-49} for each atom in the chamber. The nominal volume of interaction is about 2000 cm^3 (30 cm long and roughly 8 cm × 8 cm in area) so at a pressure reduced to its convenient nominal value of 7.5×10^{-7} Torr at temperature 480 mK, the number of molecules contained is about 3×10^{16}, giving a total scattering intensity ratio of 3.49×10^{-33}. There are 1.51×10^{26} photons produced per second in the 10^3 W, 10 GHz GB nominal case. Therefore, in 10^3 s of observation time, the estimated number of photons received from Rayleigh scattering in the interaction volume is $(3.49 \times 10^{-33})(1.51 \times 10^{26})(1000) = 5.3\times10^{-4}$ and will be negligible.

4.2 *Noise generated by diffraction*

Diffraction can potentially produce x-directed photons from a z-directed wave such as the GB in the absence of any GW interactions. This is potentially a problem for the Li-Baker detector design because the diffracted signal may either swamp the microwave receivers or else will represent a significant extraneous source of shot noise. Therefore, all sources of diffraction should be eliminated or at least minimized [54, 55]. For example, the corners at **B** and **B′** of Fig. 5

should have radii of curvature in excess of two wavelengths (6 cm) and all small obstructions and corners should have radii greater than three wavelengths (e.g., 9 cm) and the *only edge* of the focusing reflector at **A** will have **i**ts diffracted waves absorbed prior to reaching the receivers. In spite of this, there will be some microwave diffraction photon noise that will need to be reduced before reaching the receivers. Since there is *no direct path perpendicular to the GB to the microwave receivers in the x direction or from the edges of the reflectors*, due to the Herschelian optical telescope design, all x-directed photons (moving perpendicular to the axis of the GB as computed in [56]) and all diffracted photons from the reflector edge will necessarily encounter a wall of the detection chamber *before* reaching the receivers.

The number of diffraction photons emanating radially from the GB, including the effect of polarization alignment (one percent reduction), is given by equation (13) of [56]

$$n_{dif} = k^2 \left((d/2)^2/(32\, L_d^2)\right) \exp(-\tfrac{1}{2}k^2\, [d/2]^2)(0.01)\, n_{GB} \qquad (4.3a)$$

where $k = 2\pi\, \nu_e/c$ (nominally, 209 rad/m at 10GHz), c being the speed of light, the diameter of the GB throat is d (~ 0.09 m for the nominal case, essentially $2W$) and n_{GB} is the GB photon flux (nominally, 1.51×10^{26} photons per second). We will assume a single bounce or wave reflection of this diffraction-noise wave from the detector walls. The diffraction photon-path distance, prior to reaching the receivers, is L_d (~1 m for the nominal case).The number of diffraction photons, n_{dif}, moving radially will be almost evenly spread out on an area of a band of a cylinder the width of which is the length of the GB, l (~0.3 m for the nominal case), having a spread of $\pi\, L_d$. Thus the number of diffracted noise photon impinging on each receiver per second, n_{rdif} is given by

$$n_{rdif} = \quad n_{dif}\, [a_r/(l\, \pi\, L_d)]\, \varepsilon_{ab} \qquad (4.3b)$$

where ε_{ab} is the wall absorption coefficient (e.g., for the nominal case to be discussed below, it would be 10^{-22}) and a_r = area of the square receiver horn or receiving surface (nominally, one HFRGW wavelength square or 9×10^{-4} m^2).

The chamber wall absorbers are of two types: metamaterial or MM absorbers, which have no reflection, only transmission [57] at the base frequency and the usual commercially available absorbers in which there is reflection, but no transmission. In theory, multiple layers of metamaterials could result in a near "perfect" absorber (two MM layers absorbs noise to 99.9972% or –45.5 dB over their specific base frequency range 5 to10 GHz, according to the experimental data of Landy, et al. (page 3 of [57**]**). An absorbent "mat" combination of MMs (sketched as blue lines in Figs. 3, 5 and 6) backed up by commercially available microwave absorbers is shown in Fig. 8 (Patent Pending). As Landy, et al. [57**]** state in Physical Review Letters: "In this study, we are interested in achieving (absorption) in a single unit cell in the propagation direction. Thus, our MM structure was optimized to maximize the [absorbance] with the restriction of minimizing the thickness. If this constraint is relaxed, impedance matching is possible, and with multiple layers, a *perfect* [absorbance] can be achieved." We analyze an absorption mat (Patent Pending) consisting of two double MM layers, each double layer having a -45 dB absorption. Behind the MM layers is a sheet of 10 GHz tuned microwave pyramid absorbers, providing –40 dB absorption (guaranteed) before reflection back into the MM layers. Thus the total absorption is -45 -45 -40 -45 -45 = -220 dB or an absorption coefficient of 10^{-22} for the two double MM layers. There are several commercially available pyramid microwave absorbers available that offer the required low reflectivity, such as ARC Technologies, Cummings Microwave and the ETS Lindgren Rantec microwave absorbers. The ETS Lindgren

EHP-5PCL absorbing pyramids seem like a good choice. At normal incidence the typical reflectivity is down –45 dB (guaranteed –40 dB). It is also important to note that the *incident ray can have almost any inclination.* As Service writes in his article published in SCIENCE [58] "… Sandia Laboratories in Albuquerque, New Mexico are developing a technique to produce metamaterials that work with [electromagnetic radiation] coming from virtually any direction."

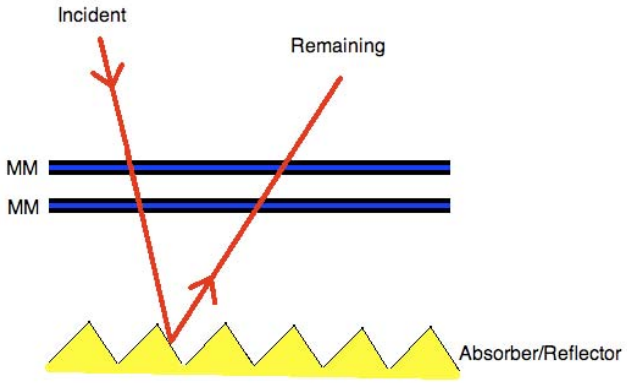

Figure 8. Schematic of typical multilayer metamaterial (two in the nominal case shown) or MM absorbers and pyramid absorber/reflector. Patent Pending.

In Tables 4, 5 and 6 are to be found a parametric analysis of the diffraction photons per second and noise equivalent power (NEP) for three alternative configurations of detector-wall absorbent mats, for GB aperture diameters, *d,* of 2, 3 (nominal) and 4 GB microwave wavelengths (6, 9, and 12 cm) and for single-reflection diffraction path lengths, L_d, of 0.5, 1.0 (nominal) and 2.0 m from the GB throat to the receivers. These distances are approximately the distance along the x-axis of the microwave receivers from the axis of the GB.

Table 4. Diffraction photons s^{-1} and NEP W for a mat composed of absorbent microwave pyramids only, exhibiting an absorption of -40 dB.

GB aperture diameter	L_d = ***0.5 m***	L_d = ***1.0 m*** (nominal)	L_d = ***2.0m***
d = **6cm**	$3.4\times10^{6}s^{-1}$,2.3×10^{-17}W	$4.3\times10^{5}s^{-1}$,3×10^{-18}W	$5.3\times10^{4}s^{-1}$,4×10^{-19}W
d = **9 cm** (nominal)	$3.3\times10^{-4}s^{-1}2.2\times10^{-27}$W	$4.2\times10^{-5}s^{-1}$,2.8×10^{-28}W	$5.2\times10^{-6}s^{-1}$,3.5×10^{-29} W
d =**12 cm**	$1\times10^{-18}s^{-1}$,7×10^{-42}W	$1.3\times10^{-19}s^{-1}$,8.7×10^{-43}W	$1.6\times10^{-20}s^{-1}$,1×10^{-43}W

Table 5. Diffraction photons s^{-1} and NEP W for absorbent microwave pyramids and one MM layer (one layer of two MMs), exhibiting an absorption of -130 dB.

GB aperture diameter	L_d = ***0.5 m***	L_d = ***1.0 m*** (nominal)	L_d = ***2.0m***
d = **6cm**	3.4×10^{-3} s^{-1}, 2.3×10^{-26} W	$4.3\times10^{-4}s^{-1}$,3×10^{-27}W	$5.3\times10^{-5}s^{-1}$,4×10^{-28}W
d= **9 cm** (nominal)	3.3×10^{-13},$s^{-1}2.2\times10^{-36}$W	$4.2\times10^{-14}s^{-1}$,2.8 10^{-37}W	$5.2\times10^{-15}s^{-1}$,3.5×10^{-38} W
d =**12 cm**	1×10^{-27} s^{-1}, 7×10^{-51}W	$1.3\times10^{-28}s^{-1}$,8.7×10^{-52}W	$1.6\times10^{-29}s^{-1}$,1×10^{-52}W

Table 6. Diffraction photons s^{-1} and NEP W for absorbent microwave pyramids and four (two layers of two) MM layers (*nominal*), exhibiting an absorption of -220 dB.

GB aperture diameter	L_d = ***0.5 m***	L_d = ***1.0 m*** (*nomina*l)	L_d = ***2.0m***
d = **6cm**	3.4×10^{-12} s^{-1}, 2.3×10^{-35} W	$4.3\times10^{-13}s^{-1}$,3×10^{-36}W	$5.3\times10^{-14}s^{-1}$,4×10^{-37}W
d = **9 cm** (*nomina*l)	3.3×10^{-22},$s^{-1}2.2\times10^{-45}$W	**$4.2\times10^{-23}s^{-1}$,2.8 10^{-46}W**	$5.2\times10^{-24}s^{-1}$,3.5×10^{-47} W
d =**12 cm**	1×10^{-36} s^{-1}, 7×10^{-60}W	$1.3\times10^{-37}s^{-1}$,8.7×10^{-61}W	$1.6\times10^{-38}s^{-1}$,1×10^{-61}W

Note that if during prototype-detector tests it became apparent that diffraction rays reached a microwave receiver without being intercepted by an absorbent wall, then one would increase the diameter of the nominal or design GB from 9 cm to 12 cm resulting in diffraction flux at a receiver of 1.31×10^{-15} s^{-1}, which would be negligible. Such a design change would also increase detector size and cost, so this alternative design would not be pursued unless needed.

4.3 *Noise generated by thermal photons*

In addition, isolation from background noise is further improved by cooling the microwave receiver apparatus to reduce thermal noise background to a negligible amount. A cooling system is selected so that the temperature T satisfies $k_BT << \hbar\omega$, where k_B is Boltzmann's constant and $\boldsymbol{T} << \hbar\omega/k_B \approx$ 480mK for detection at 10 GHz and for the detector's narrow bandwidth. This condition is satisfied by the target temperature for the detector enclosure $T <$ 480mK, which can be conveniently obtained using a common helium-dilution refrigerator so that virtually no thermal photons will be radiated at 10 GHz.

4.4 *Comprehensive noise summary*

A standard sensor design method, already mentioned, for aggregating noise sources is to translate all noise terms through the system, or "refer them" from the location at which they occur to the equivalent noise at the detection photon microwave receiver(s) [51]. Such an expression of noise is equivalent to the amount of power that this amount of noise would represent at the detector, and is known as the noise-equivalent power or NEP. All the uncorrelated noise components can be root-sum-squared together, so that:

$$\text{NEP} = \sqrt{[\ (P_{nd})^2 + (P_{ns})^2 + (P_{nj})^2 + (P_{npa})^2 + (P_{nqa})^2]}\ \text{W} \quad , \tag{4.4}$$

where the equivalent-power noise components are defined as follows:

The *dark-background shot noise is* $P_{nd} = \hbar\nu\sqrt{(N_d)}/\Delta t$ and N_d is the dark-background-photon count. Shot noise is proportional to the square root of the number of photons present in a sample and is mitigated by using the absorption layers on the detector walls and wall geometry (Herschelian telescope geometry) to keep the microwave receivers "below" and "out of sight" of the GB entry-aperture source of diffraction and all *x-directed* diffraction from the GB kept "above" and not directed to the receivers as shown in Fig. 5. (The x-directed diffraction from the

GB move in planes parallel to the x-y plane.) Tables 4-6 present the calculated diffraction with the nominal design given in Table 5. Stray BPF spillover and diffraction that still manages to get reflected onto the detectors will create the shot noise, but such noise could be filtered out by pulse-modulating the magnetic field and a baffle arrangement shown in Fig. 8.

The *signal shot noise is* $P_{ns} = \hbar\, \nu\sqrt{(N_s)}/\Delta t$ where N_s is the signal-photon count, and Δt is the sample or accumulation time. This "noise" is part of the useful data and should not to be subject to elimination.

The *Johnson noise* (due to the thermal agitation of electrons when they are acting as charge carriers in a power amplifier) is $P_{nj} = 4k_B T R_L B_W$, where R_L is the equivalent resistance of the front-end amplifier and B_W is the bandwidth. Mitigation of this noise source is accomplished by reducing bandwidth or reducing load resistance. However, in practice the bandwidth is often fixed by the application, in this case by the detection bandwidth. And the load resistance is required to generate a large voltage from a very small current. Hence there is in practice an optimum selection of load resistance that will optimize the signal to noise output during the initial tests of the Li-Baker detector, and the selection of this load resistance is the essence of impedance matching in its most basic form. Johnson noise is generally reduced or eliminated by refrigeration to 0.48K. At a B_w of 0.001 Hz and a sample interval of Δt =1000 seconds the noise is 3.37×10^{-28} W or 5×10^{-5} noise photons per second [59].

The *preamplifier noise* is $P_{npa} = B_w/ f_1$, which is essentially 1/f noise, where the crossover frequency f is related to stray capacitance and load resistance; in which $f_1 = 1/(2\pi R_L C_{jn})$, where C_{jn} = detection capacitance plus FET (field effect transistor) input capacitance plus stray capacitance. This noise source is mitigated by reducing bandwidth, reducing load resistance, or reducing stray capacitance. From [60] at a B_w of 0.001 Hz and a sample interval of Δt =1000 seconds the noise is 7.57×10^{-30} W or 1.13×10^{-6} noise photons per second.

The *quantization noise* is $P_{nqa} = QSE/\sqrt{12}$, where QSE is the quantization step equivalent or the value of one LSB (Least Significant Bit , the smallest value that is quantized by an ADC, or Analog to Digital Converter). This noise source is easily mitigated and eliminated by increasing the number of bits used in an ADC so that the LSB is a smaller portion of the overall signal. In practice the QSE is selected so that it does not cause lower SNR. The noise is 1.33×10^{-26} W or 2×10^{-3} noise photons per second.

The *mechanical thermal noise* is caused by the Brownian motion of sensor components. Mitigation is to refrigerate the sensing apparatus to reduce thermal inputs. The 0.48 K cooling should be sufficient, but if not an even lower temperature can be achieved. [61]

The *phase* or *frequency noise* (of the EM-GB) is due to the fluctuations in the frequency of the microwave source for the GB. Steps will need to be taken during the Li-Baker detector tests to keep the GB source tuned precisely to the interaction volume resonance, thus reducing phase noise and maximizing the resonant magnification effect required from the interaction volume cavity. A cavity-lock loop or alternatively a phase-compensating feedback loop will be selected during post-fabrication trials to mitigate this noise source

The noise or noise equivalent power at the receiver(s) or NEP as summarized in Table **7**, is not a constant, but exhibits a stochastic or random component. In order to obtain the best estimate of the detection photons, one would need to utilize a filter, possibly a Kalman filter [62].

Table 7. Summary of Li-Baker detector noise for nominal case.

Noise Contributor	**Brief Description of Noise source**	**Mitigation/Elimination Means**	**Nominal Computed Value photons s^{-1}, NEP W**
Dark-background shot noise	GB noise especially diffraction	Wall geometry and absorbing wall materials	$4.2\times10^{-23}s^{-1}$,2.8 10^{-46}W
Signal shot noise	Noise in the signal itself	Part of useful data and not to be eliminated	--
Johnson noise	Thermal agitation in a power amplifier resistance	Refrigeration to low temperature	$5\times10^{-5}s^{-1}$,3×10^{-28} W
Preamplifier kTC noise	Stray capacitance and load resistance	Reducing bandwidth, load resistance and/or stray capacitance.	$1\times10^{-6}s^{-1}$, 8×10^{-30} W
Quantization noise	Analog to Digital Converter	Increasing the number of bits used	$2\times10^{-3}s^{-1}$, 1×10^{-26} W
Mechanical thermal noise	Brownian motion of sensor components.	Refrigeration to low temperature	$3\times10^{-4}s^{-1}$,2×10^{-27} W
Phase or *Frequency noise*	Fluctuations in the frequency of the microwave source for the GB.	Cavity-lock loop or a phase-compensating feedback loop	$5\times10^{-15}s^{-1}$,3×10^{-38} W

The total NEP from Eq. (4.4) of 1.02×10^{-26} W (noise flux is 1.54×10^{-3} photons per second) is Quantization and thermal noise limited at roughly 1×10^{-26} to 2×10^{-27} W for a detector temperature of 0.48K. If need be the receivers could be further cooled and shielded from noise by baffles [54] as shown in Fig. 9 in which the spherical BPF wave front, if significant, can be reduced by baffle diffraction and the PPF focused by the reflectors passed through the baffle openings with less interaction with baffle edges and less diffraction. Given a signal that exhibits the nominal value given in Table 2 of 99.2 s^{-1} photons, one quarter of which is focused on each of the microwave receivers, which is 24.8 s^{-1} photons or 1.6×10^{-22} W, the signal-to-noise ratio for each receiver is better than 1500:1.

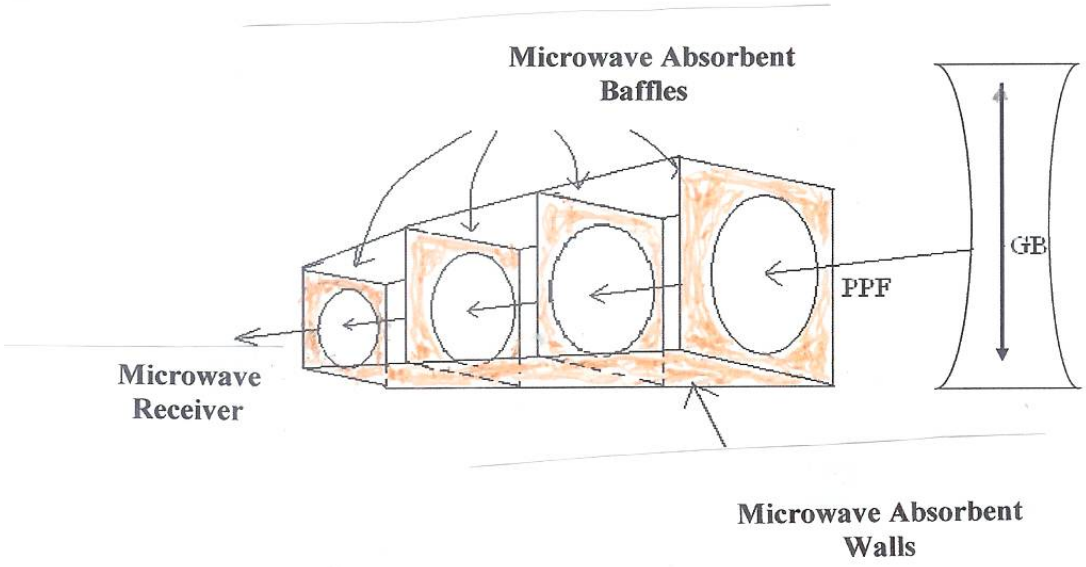

Figure 9. Schematic of microwave receiver shielded by MM absorbers and pyramid absorber/reflectors.

4.5 *Noise mitigation by magnetic-field modulation*

As noted, a unique feature of the Li-Baker HFGW detector is that some of the noise sources are present when the magnetic field is "off" and there is no signal or detection photons present. With the magnetic field "on" there is noise plus the signal. Thus, one can distinguish between HFRGW generated photons and the background generated photons from the GB. In principle one could use coincidence gating to subtract the "noise" (with the magnet "off") from the "signal plus noise" with the magnet "on" and obtain the signal alone. However, there will still be stochastic noise sources that form a noise spectrum that can be reduced by filtering but cannot be completely removed. Consider a simplified case of a uniform, low-frequency (compared with the 10 GHz signal) square-wave chopper frequency energizing the magnet, with the magnet alternatively "off" and "on." It could be utilized to remove some of the background photons from the GB.

4.5 *Standard quantum limit (SQL)*

There is another possible concern here: Stephenson [63] concluded that a HFRGW intensity of $h_{det} = 10^{-30}$ to 10^{-32}m/m (strain in the fabric of space-time whose amplitude is A) represent the lowest possible GW strain variations detectable by each RF receiver in the Li-Baker HFGW detector. There is a limit to this sensitivity that is called "quantum back-action" or standard quantum limit (SQL) and is a result of the Heisenberg uncertainty principle [64]. An additional $(1/\sqrt{2})$ factor increase in maximum sensitivity applies if the separate outputs from the two RF receivers are averaged, rather than used independently for false alarm reduction, resulting in a minimum $h_{det} = 1.2\times10^{-37}$. Because the predicted best sensitivity of the Li-Baker detector in its currently proposed configuration is $A = 10^{-30}$m/m, these results confirm that the Li-Baker detector is photon-signal-limited, not quantum-noise-limited; that is, the SQL is so low that a properly designed Li-Baker detector can have sufficient sensitivity to observe HFRGW of

amplitude $A \approx 10^{-30}$ m/m or less. In theory the Li-Baker detector is about seven orders of magnitude less sensitive than the standard quantum sensitivity limit.

4.6 Sensitivity *increase*

It may be desirable to increase the sensitivity of the prototype Li-Baker detector through use of more sensitive microwave receivers, a stronger magnetic field, a more powerful microwave GB transmitter, a larger interaction volume, the introduction of resonance chambers, etc.; but even if one cannot greatly increase sensitivity immediately, a null experimental result would still be valuable, since it can provide the indirect means to determine whether or not some theories and scenarios should be corrected or eliminated. For example, the data analysis of low-frequency, laser-interferometer gravitational-wave detectors, such as LIGO and Virgo [65], have so far had null results, but have been the basis for cosmological theory improvements and have had important significance for further study.

5. Conclusions

Three HFGW detectors have previously been fabricated and two others theoretically proposed, but analyses of their sensitivity and the results provided herein suggest that for meaningful relic gravitational wave (HFRGW) detection, greater sensitivity than those instruments currently provide is necessary. The theoretical sensitivity of the Li-Baker HFGW detector studied herein, and based upon a different measurement technique than the other detectors, is predicted to be $A = 10^{-30}$ m/m at base frequencies near to 10 GHz. This detector design is not quantum-limited and theoretically exhibits sensitivity sufficient for useful relic gravitational wave detection. Utilization of magnetic-field pulsed modulation allows for reduction in some types of noise. Other noise effects are found theoretically to be minimal; but they can only be accurately determined based on the Li-Baker prototype detector tests and some of the design and adjustments can only be finalized during prototype fabrication and testing. The detector can be built from off-the-shelf, readily available components and its research results would be complementary to the proposed low-frequency gravitational wave (LFGW) detectors, such as the Advanced LIGO and the proposed Laser Interferometer Space Antenna or LISA.

Acknowledgments

This work is supported by the National Nature Science Foundation of China under Grant No. 11075224, the Foundation of China Academy of Engineering Physics under Grant Nos. 2008T0401 and 2008T0402, Chongqing University Postgraduates Science and Innovation Fund No. 200811B1A0100299, GravWave® LLC, Transportation Sciences Corporation and Seculine Consulting. All authors reviewed, edited and approved the manuscript. Some material by RCW was based on work supported by the US National Science Foundation, while working at the Foundation. Any opinion, finding, and conclusions or recommendations expressed in this material are those of the authors and do not necessarily reflect the views of the US National Science Foundation. FYL initially developed the theory; RMLBjr designed the microwave-absorbing baffles and the reflectors including the off-axis Herschelian telescope and the exterior to GB focusing lenses to reduce diffraction noise, suggested the use of the vacuum and the utilization of two microwave detectors, AWB developed the astrophysical applications, RCW analyzed the magnet and Gaussian beam scattering, GVS developed the standard quantum limit and the noise equivalent power approach and RCW and GVS developed the concept for the high-sensitivity microwave receivers and signal processing. Christine S. Black provided the figures and Amara D. Angelica edited the manuscript.

Appendix

Brief summary of the Li-effect proof

This detector is a coupling system among Gaussian-type microwave photon flux, a static magnetic field and fractal membranes (or other equivalent microwave optics) [31, 32, 37, 38]. Unlike the pure-inverse Gertsenshtein effect (G-effect), here under the synchro-resonance condition, coherence modulation of the HFGWs to the preexisting transverse photon flux of the Gaussian beam (GB) is predicted to produce the transverse (radial) first-order perturbative photon flux (PPF) or signal due to the presence of GWs as shown in Fig. 1A, and the PPF has a maximum at a longitudinal symmetrical surface of the GB where the transverse background photon flux (BPF) or GB noise vanishes. Moreover, the PPF and the BPF have obviously different decay rates in the transverse direction, and the PPF reflected, for example by the fractal membranes, exhibits a very small decay to be compared with a very large decay of the much stronger BPF. Thus, such properties might provide a new way to distinguish the BPF (noise) and display the PPF (signal). The general form of the GB of a fundamental frequency mode is [43]

$$\psi = \frac{\psi_0}{\sqrt{1+(z/f)^2}} \exp\left(-\frac{r^2}{W^2}\right) \exp\left(i\left[(k_e z - \omega_e t) - \tan^{-1}\frac{z}{f} + \frac{k_e r^2}{2R} + \delta\right]\right) \quad \text{(A1)}$$

where $r^2 = x^2 + y^2$, $k_e = 2\pi/\lambda_e$, $f = \pi W_0^2/\lambda_e$, $W = W_0\sqrt{1+(z/f)^2}$, $R = z + f^2/z$, ψ_0 is the amplitude of the electric (or magnetic) field of the GB, W_0 is the minimum spot radius, R is the curvature radius of the wave front of the GB. From Eq. (A1) one finds [37, 38]

$$n_x^{(0)} = f_x^{(0)} \exp\left(-\frac{2r^2}{W^2}\right),\ n_y^{(0)} = f_y^{(0)} \exp\left(-\frac{2r^2}{W^2}\right),\ n_z^{(0)} = f_z^{(0)} \exp\left(-\frac{2r^2}{W^2}\right) \quad \text{(A2)}$$

where $n_x^{(0)}$, $n_y^{(0)}$, $n_z^{(0)}$ represent the average values in the x-, y- and z- directions of the BPF (noise) and $f_x^{(0)}\big|_{x=0} = f_y^{(0)}\big|_{y=0} = 0$, $f_z^{(0)}\big|_{x=y=0} = f_z^{(0)}\big|_{z\max}$. Because of the non-vanishing $n_x^{(0)}$ and $n_y^{(0)}$, the GB will be asymptotically spread as $|z|$ increases.

Unlike $n_x^{(0)}$, $n_y^{(0)}$ and $n_z^{(0)}$ (noise), the PPF $n_x^{(1)}$, $n_y^{(1)}$ and $n_z^{(1)}$ (signal) have different decay forms:

$$n_x^{(1)} = f_x^{(1)} \exp\left(-\frac{r^2}{W^2}\right),\ n_y^{(1)} = f_y^{(1)} \exp\left(-\frac{r^2}{W^2}\right),\ n_z^{(1)} = f_z^{(1)} \exp\left(-\frac{r^2}{W^2}\right) \quad \text{(A3)}$$

where $f_x^{(1)}$, $f_y^{(1)}$ and $f_z^{(1)}$ are the functions of position *x, y, z*. Therefore, the decay rate of $n^{(1)}$ (signal) is slower than that of $n^{(0)}$ (noise).

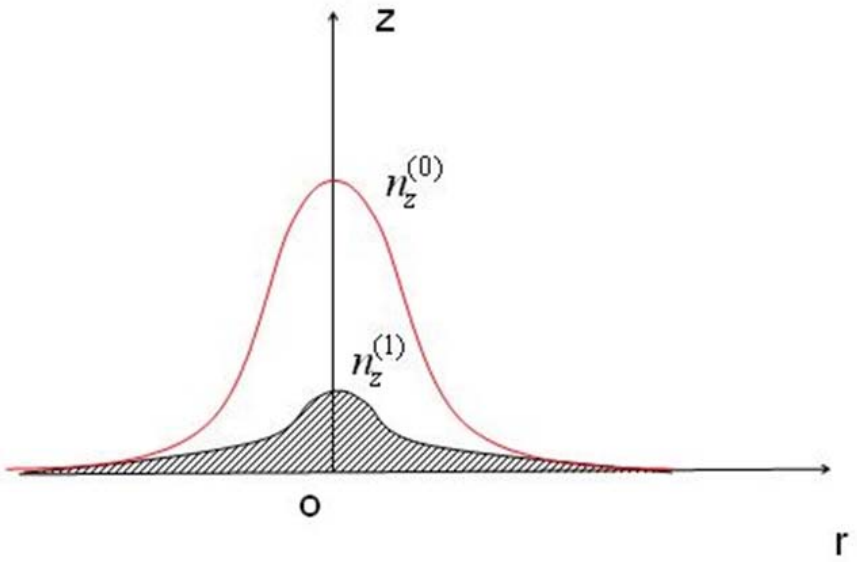

Figure.1A. First-order longitudinal PPF ($n_z^{(1)}$ signal) and BPF ($n_z^{(0)}$ noise) in the Li-Baker detector in the z direction as measured radially, r .

In the Li-Baker detector the first-order longitudinal PPF $n_z^{(1)}$ and the BPF $n_z^{(0)}$ have the same propagating direction, and $n_z^{(0)}$ is much lager then $n_z^{(1)}$ in most of the nearby regions. Thus, $n_z^{(1)}$ will be swamped by the $n_z^{(0)}$ in such regions. However, the $n_z^{(1)}$ and $n_z^{(0)}$ will exhibit a comparable order of magnitude in the "far-axis region" (r >30cm about the distance of 6 spot radii of the GB as shown in Fig. 2A) due to the different decay rates and the $n_z^{(1)}$ will become larger than $n_z^{(0)}$ further out in the radial, r, direction. Therefore, as discussed in Section 4, the Li-Baker detector is photon-signal-limited, not quantum-noise limited.

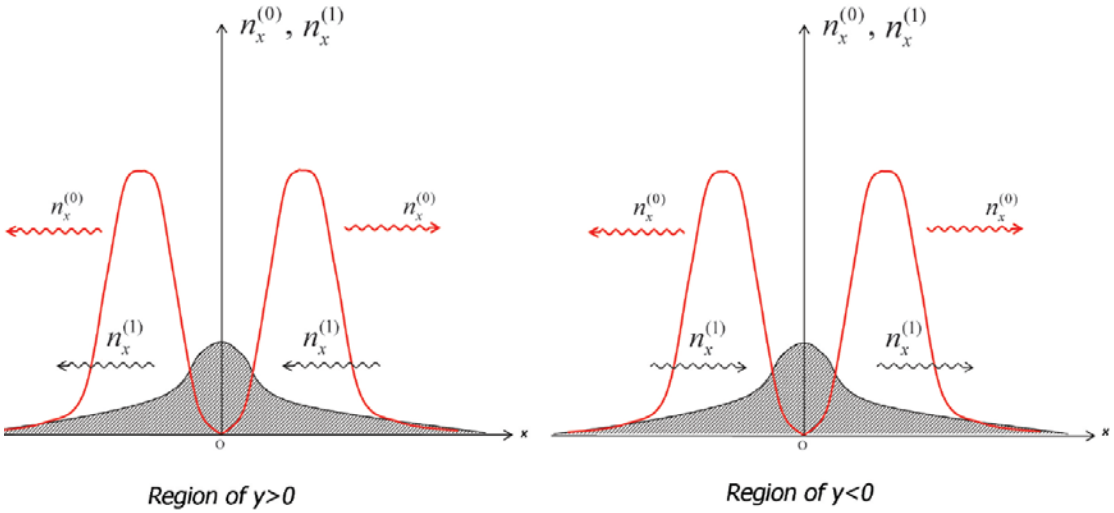

Figure 2A. Schematic diagram of strength distribution of the transverse BPF $n_x^{(0)}$ and PPF $n_x^{(1)}$ in the outgoing wave region of the GB [32, 33].

Unlike Fig.1A, here $n_x^{(0)}\big|_{x=0} = 0$ while $n_x^{(1)}\big|_{x=0} = n_{x\max}^{(1)}$. Thus, $n_x^{(1)}\Delta t$ (accumulated signal) can be effectively larger than the background noise photon fluctuation $\left(n_{xtot}^{(0)}\Delta t\right)^{1/2}$ at the yz-plane and at the parallel surfaces near the yz-plane, provided that the total noise photon flux passing through the surface can be effectively suppressed as discussed in Section 4. Because $n_x^{(1)}$ propagates along apposite directions in the regions of *y>0* and *y<0* in the GB, there is conservation of total momentum in the coherent resonance interaction and there is also an ability to focus half of the $n_x^{(1)}$, which are directed to the center of the GB, at the two microwave receivers at opposite ends of the x-axis. The reverse mirror image of Fig. 2A in the xy-plane (z < 0) insures that there is conservation of angular momentum and the differentiation of the interaction volume into octants about the origin (center or intersection of the axes of the GB and the static magnetic field) is established by [37, 38].

References

1. Abbott B P, et al 2009 An upper limit on the stochastic gravitational-wave background of cosmological origin The LIGO Scientific Collaboration & The Virgo Collaboration *Nature* **460** 991
2. Krauss M, Scott D and Meyer S 2010 Primordial gravitational waves and cosmology *Science* **328** 989-992
3. Mensky M B 1975 On gravitational-electromagnetic resonance, *Problems of the theory of gravity and elementary particles* Issue 6 ed .K P Stanyukovich (Moscow, Atomizdat) pp. 181-190
4. Mensky M B and Rudenko V N 2009 High-frequency gravitational wave detector with electromagnetic-gravitational resonance *Gravitation and Cosmology* **1** 167-170
5. Einstein A 1915 Die Feldgleichungen der gravitation Sitzungsberichte der Preussischen Akademie der Wissenschaften zu Berlin. 844–847, http://nausikaa2.mpiwg-berlin.mpg.de/cgi bin/toc/toc.x.cgi?dir=6E3MAXK4&step=thumb
6. Brustein R, Gasperini M, Giovannini M and Veneziano G 1995 Relic gravitational waves from string cosmology *Phys. Lett. B.* **361** 45
7. Buonanno A, Maggiore M and Ungarelli C 1997 Spectrum of relic gravitational waves in string cosmology *Phys. Rev. D.* **55** 03330
8. de Vega H J, Mittelbrünn J R and Sanchez M 1999 Generation of gravitational waves by generic sources in De Sitter space-time *Phys. Rev. D.* **60** 04407
9. Giovannini M 1999 Production and detection of relic gravitons in quintessential inflationary models *Phys. Rev. D.* **60** 01235
10. Grishchuk L P 1999 Proc. 34th Rencontres de Moriond: Gravitational Waves and Experimental Gravity
11. Beckwith A W 2009 Relic high frequency gravitational waves from the big bang and how to detect them Proceedings of the Space, Propulsion and Energy Sciences International Forum (SPESIF) American Institute of Physics Conference Proceedings **1103** ed G Robertson (Melville, NY) p. 571
12. Infante M P and Sanchez N 2000 The primordial gravitation wave background in string cosmology *Phys Rev D* **61** 083515

13. Mosquera-Cuesta H J and Gonzalez, D M 2001 Bursts of gravitational radiation from superconducting cosmic strings and the neutrino mass spectrum *Phys .Lett. B* **500** 215-221
14. Bisnovatyi-Kogan G S and Rudenko V N 2004 Very high frequency gravitational wave background in the universe *Class. Quantum Grav.* **21** 3347-3359
15. Shawhan, P. S.: Gravitational waves and the effort to detect them. American Scientist **92**, 4, 350-356 (2004)
16. Beckwith A W 2010 How to use the Cosmological Schwinger Principle to predict energy flux, entropy and an effective electric field at the start of Inflation in terms of Inflation potentials http://vixra.org/abs/1009.0020
17. Grishchuk L P 1976 Primordial gravitons and the possibility of their observation. *JETP Lett.* **23** 293
18. Grishchuk L P 1977 Gravitational waves in the cosmos and the laboratory *Sov. Phys. Usp* **20** 319
19. Grishchuk L P 1988 Gravitational-wave astronomy *Sov. Phys. Usp* **31** 940
20. Grishchuk L P 2006 Relic gravitational waves and cosmology arXiv:gr-qc/0504018v4
21. Garcia-Cuadrado G 2009 Towards a new era in gravitational wave detection: high frequency gravitational wave research Proceedings of the Space, Propulsion and Energy Sciences International Forum (SPESIF) American Institute of Physics Conference Proceedings **1103** ed G Robertson (Melville, NY) pp. 553-563 [http://www.gravwave.com/docs/Toward%20a%20New%20Era%20in%20Gravitational%20Wave%20Research.pdf]
22. Douglass D H and Braginsky B 1979 Gravitational-radiation experiments in General relativity: an Einstein centenary survey ed Hawking S W and Israel W (CUP, UK) pp. 90-137
23. Cruise A M 2000 An electromagnetic detector for very-high-frequency gravitational waves *Class. Quantum Grav.* **17** 2525-2530
24. Cruise A M and Ingley R M J 2005 A correlation detector for very high frequency gravitational waves *Class. Quantum Grav.* **22** 5479-5481
25. Bernard P, Gemme G, Parodi R and Picasso E 2001 A detector of small harmonic displacement based on two coupled microwave cavities *Review of Scientific Instruments* **72** 5 2428-2437
26. Chincarini A and Gemme G 2003 Micro-wave based high-frequency gravitational wave detector paper HFGW-03-103 Gravitational-Wave Conference The MITRE Corporation
27. Ballantini R, et al 2005 Microwave apparatus for gravitational waves observation INFN Technical Note INFN/TC-05/05, gr-qc/0502054
28. Nishizawa A, et al 2008 Laser-Interferometric detectors for gravitational wave backgrounds at 100 MHz: detector design and sensitivity *Phys. Rev. D* **77** Issue 2 022002
29. Li F Y, Tang M and Zhao P 1992 Interaction between narrow wave beam-type high frequency gravitational radiation and electromagnetic fields *Acta Physica Sinica* **41** 1919-1928
30. Li F Y, Tang M X, Luo J and Li Y C 2000 Electrodynamical response of a high energy photon flux to a gravitational wave *Phys. Rev. D* **62** 044018-1
31. Li F Y and Tang M X 2002 Electromagnetic detection of high-frequency gravitational waves *International Journal of Modern Physics D* **11**(7) 1049-1059

32. Li F Y, Tang M X and Shi D P 2003 Electromagnetic response of a Gaussian beam to high-frequency relic gravitational waves in quintessential inflationary models *Physical Review D* **67** 104008-1 to -17
33. Li F Y, Wu Z H and Zhang Y 2003 Coupling of a linearized gravitational wave to electromagnetic fields and relevant noise issues *Chin. Phys. Lett.* **20** 11 1917
34. Li F Y and Yang N 2004 Resonant interaction between a weak gravitational wave and a microwave beam in the double polarized states through a static magnetic field *Chin. Phys. Lett.* **21** 11 2113
35. Li F Y and Baker R M L Jr 2007 Detection of high-frequency gravitational waves by superconductors *International Journal of Modern Physics B* **21** 18-19, 3274-3278
36. Li F Y and Yang N 2009 Phase and polarization state of high-frequency relic gravitational waves *Chin. Phys. Lett.* **26** 5 050402
37. Li F Y, Baker R M L Jr, Fang Z, Stephenson, G V and Chen Z 2008 Perturbative photon fluxes generated by high-frequency gravitational waves and their physical effects *European Phys. J. C* **56**, 407-423 [http://www.gravwave.com/docs/Li-Baker%206-22-08.pdf]
38. Li F Y, Yang N, Fang Z., Baker R M L Jr, Stephenson G V and Wen H 2009 Signal photon flux and background noise in a coupling electromagnetic detecting system for high-frequency gravitational waves *Phys. Rev. D.* **80** 060413-1-14 [arXiv: gr-qc/0909.4118] [http://www.gravwave.com/docs/Li,%20et%20al.%20PRD%2009-9-09%20.pdf]
39. Baker R M L Jr, Stephenson G V and Li F 2008 Proposed ultra-high sensitivity HFGW detector Proceedings of Space Technology and Applications International Forum (STAIF-2008) **969** ed El-Genk M S American Institute of Physics Conference Proceedings (Melville, N Y) pp. 1045-1054 [http://www.gravwave.com/docs/Proposed%20Ultra High%20Sensitivity%20HFGW%20Detector%2005-15-08.pdf]
40. Baker R M L Jr 2007 Peoples Republic of China Patent Number 0510055882.2, Gravitational Wave Generator (Detector Portion). [http://www.drrobertbaker.com/docs/Chinese%20Detector%20Patent.pdf]
41. Grishchuk L P 2007 High-frequency relic gravitational waves and their detection 2nd High-Frequency Gravitational Wave Symposium, Austin, Texas September 19 slide #6, [http://www.gravwave.com/docs/Grishchuk%20%20HFGW%20Lect.pdf] (2007)
42. Gertsenshtein M E 1962 Wave resonance of light and gravitational waves Soviet *Physics JETP* **14** 1 84-85
43. Yariv A 1975 *Quantum Electronics 2nd Ed.* (New York: Wiley)
44. Baker R M L Jr, Woods R C and Li F L 2006 Piezoelectric-crystal-resonator high-frequency gravitational wave generation and synchro-resonance detection Proceedings of Space Technology and Applications International Forum (STAIF-2008) **813** ed El-Genk M S American Institute of Physics Conference Proceedings (Melville, N Y) pp. 1280-1289
45. Eardley D 2008 High frequency gravitational waves JSR-08-506 the JASON defense science advisory panel and prepared for the Office of the Director of National Intelligence, [http://www.fas.org/irp/agency/dod/jason/gravwaves.pdf]
46. Wen W, Zhou L, Li J, Ge W, Chan C T and Sheng P 2002 Subwavelength photonic band gaps from planar fractals *Phys. Rev. Letters* **89** 22
47. Zhou L, Wen W, Chan C T and Sheng P 2003 *Phys. Rev. Letters* **82** 7

48. Yamamoto K, Tada M, Kishimoto Y, Shibata M, Kominato K, Ooishi T, Yamada S., Saida, T, Funahashi H, Masaike A and Matsuki S 2001The Rydberg-atom-cavity Axion search [arXiv:hep-ph/0101200 v1]
49. Schuster D I, Houck A, Schreier R, Wallraff A, Gambetta J M, Blais A, Frunzio L, Johnson B, Devoret M H, Girvin S M and Schoelkopf R J 2006 Resolving photon number states in a superconducting circuit [arXiv:cond-mat/0608693 v1]
50. Buller G S and Collins R J 2010 Single-photon generation and detection *Meas. Sci. Technol.* **21** 1-28
51. Boyd R. W 1983 *Radiometry and the Detection of Optical Radiation* (John Wiley & Sons, NY) pp. 10ff
52. Nave, R 2009 Rayleigh scattering http://hyperphysics.phy-astr.gsu.edu/hbase/atmos/blusky.html#c2. [Assessed July 9, 2009].
53. Robb W B 1974 The frequency dependent polarizability of atomic nitrogen *J. Phys. B: At. Mol. Phys* **7** L369
54. Keller J B 1962 Geometrical theory of diffraction **32** No. 2 *J. Opt. Soc. Am*. 116-133
55. Sheppard C J R and Hrynevych M 1992 Diffraction by a circular aperture: a generalization of Fresnel diffraction theory **A/9** No. 2 *J. Opt. Soc. Am*. February 274- 281
56. Woods R C 2011 Estimate of diffraction from Gaussian Beam in Li-Baker HFGW detector Accepted by 2011 Space, Propulsion and Energy Sciences International Forum (SPESIF2011) Proceedings of the Space, Propulsion and Energy Sciences International Forum (SPESIF) American Institute of Physics Conference Proceedings ed G Robertson (Melville, NY) http://www.gravwave.com/docs/Woods%202010.pdf
57. Landy N I, Sajuyigbe S, Mock J J, Smith D R and Padilla W J 2008 Perfect metamaterial absorber *Physical Review Letters* **100** 207402-1-4
58. Service R F 2010 Next wave of metamaterials hopes to fuel the revolution *Science* **327** 138-139
59. Tsai M D, Cho Y H and Wang H 2005 A 5-GHz Low Phase Noise Differential Colpitts CMOS VCO *IEEE microwave and wireless components Letters* **15** 327
60. Giannini F, Limiti E, Orengo G, Serino A and DeDominicis M 2002 A High Gain-Bandwidth Product Distributed Transimpedance Amplifier IC for High-Speed Optical Transmission Using Low-Cost GaAs Technology Proceedings of GAAS 2002, 23-27 September Milano. Research Contributions of the Alma Mater Studiorum – University of Bologna. [http://amsacta.cib.unibo.it/149/]
61. Planck M 1914 *The theory of heat radiation 2nd edition* (Blackiston Son & Co., Philadelphia) 13, 30, 42
62. Baker R M L Jr 1967 *Astrodynamics: Applications and Advanced Topics* (New York and London: Academic Press) pp. 376-392
63. Stephenson G V 2009 The standard quantum limit for the Li-Baker HFGW detector Proceedings of the Space, Propulsion and Energy Sciences International Forum (SPESIF) American Institute of Physics Conference Proceedings **1103** ed G Robertson (Melville, NY) pp 542-547 [http://www.gravwave.com/docs/HFGW%20Detector%20Sensitivity%20Limit.pdf]
64. Kippenberg T J, Vahala K J 2008 Cavity optomechanics: back-action at the mesoscale *Science* **321** 1172-1176

65. Abbott B, et al 2007 Searching for a stochastic background of gravitational waves with the laser interferometer gravitational wave observatory *Astrophys. J.* **659** 918-930